

<https://doi.org/10.48047/AFJBS.6.12.2024.2179-2190>



African Journal of Biological Sciences

Journal homepage: <http://www.afjbs.com>



Research Paper

Open Access

Synthesis, *Insilico* Studies and Biological Evaluation of *N*-acyl Hydrazone Derivatives

Pulagam Amrutha ¹, Donthamsetty V Sowmya ², Punyasamudram Sandhya ², Galla Rajitha ^{1,*}

¹Department of Pharmaceutical Chemistry, Institute of Pharmaceutical Technology, Sri Padmavati Mahila Visvavidyalayam, Tirupati-517502, Andhra Pradesh, India

²Department of Organic Chemistry, Sri Padmavati Mahila Visvavidyalayam, Tirupati-517502, Andhra Pradesh, India

***Correspondence:**

Prof. Rajitha Galla

Institute of Pharmaceutical Technology,
Sri Padmavati Mahila Visvavidyalayam,
Tirupati, Andhra Pradesh 517502, India.

Mail: rajitha.galla@gmail.com

Phone: +91-9441882891

Article History

Volume 6, Issue 12, 2024

Received: 30 May 2024

Accepted: 30 June 2024

Doi:

10.48047/AFJBS.6.12.2024.2179-2190

Abstract

N-acyl hydrazides are highly intriguing to medicinal chemists due to their extensive range of biological actions. Many nonsteroidal anti-inflammatory drugs (NSAIDs) available on the market are limited, and the potential risks related to the inflammation process provide an immense challenge for medicinal chemists to discover more effective anti-inflammatory drugs. In the present work, a variety of *N*-acyl hydrazone derivatives were prepared by a dual-step reaction. Cyanoacetohydrazone, 2-hydroxy-1-naphthaldehyde, Ethanol, pyridine, substituted benzaldehydes, Glacial acetic acid are used for the synthesis. Characterization was performed by UV, IR, and NMR spectral techniques. Then the potential of these compounds against the COX-2 receptor for anti-inflammatory activity was analyzed using the *insilico* method. Carrageenan-induced Paw Edema method was used for *in vivo* anti-inflammatory activity. The antioxidant activity of the compounds was evaluated by DPPH and nitric oxide assays. The compound **4e** exhibited an equivalent but marginally superior docking score than the standard celecoxib whereas compounds **4d**, **4f** and **4g** displayed comparable docking scores. Molinspiration studies revealed that there are no Lipinski violations in all the synthesized compounds. The trimethoxy derivative (**4d**) has anti-inflammatory activity similar to celecoxib, while the dimethoxy (**4e**), 2-hydroxy-3-methoxy (**4g**), and 4-hydroxy (**4f**) derivatives showed good anti-inflammatory activity. Among all the compounds, **4g** showed good antioxidant activity in both assays, with 71% and 56% inhibition.

Key Words: Hydrazides,

insilico, anti-inflammatory, antioxidant, carrageenan-induced paw edema

Introduction

Hydrazides represent a diverse class of organic compounds that are formed from hydrazine and are characterized by a covalent bond between two nitrogen atoms and the presence of at least one acyl substituent (Zarafu et al., 2020). As far back as 1895, Kurzius synthesized the very first hydrazide representatives of formic acid and acetic acid Smith(1951). Hydrazides represent the functional group $-C(=O)NHNH_2$. The hydrazine moiety provides hydrazides with intriguing chemical properties, such as their ability to undergo hydrazone formation, which involves the hydrazide reacting with carbonyl compounds (Ken-Ichi et al., 2015). These compounds and their derivatives serve as building blocks in the synthesis of various heterocycles that contain one or more heteroatoms and have a variety of pharmaceutical applications Elnagdi and Erian(1991). Figure 1 shows some popularly marketed drugs containing a hydrazide moiety.

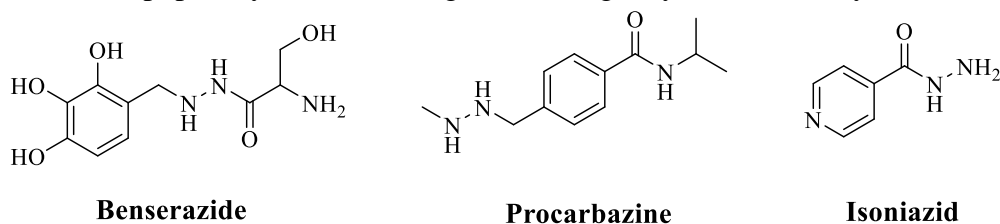


Figure 1. Marketed drugs with hydrazide moiety

The wide spectrum of biological activities that different hydrazide analogues possess (Sambrajyam et al., 2022; Soujanya and Rajitha, 2017; Hegira et al., 2021; Wagdy, et al., 2015; Vikramjeet, et al., 2013; Vikas, et al., 2012) has inspired us to design novel hydrazides and explore their pharmacological potential. In the present work, the Schiff bases of 2-hydroxy-1-naphthaldehyde were reacted with substituted benzaldehydes, waving to the biological significance of the former (Zahid and Hazoor, 2008; Sarah et al., 2016; Neelofar et al., 2018; Bhagwat et al., 2022). In the modern medical era, the integration of computational knowledge and expertise from organic chemists has accelerated the drug development process. In order to synthesize the potential hydrazides, we subjected the title derivatives to ADMET identification to ensure safety and drug likeness of the compounds. With the aim to develop a potent novel hydrazide, the synthesized molecules were screened for biological evaluation in three major therapeutic areas, which can become a break-through for many other interconnected disorders in future.

Materials and Methods

Materials

All the chemicals and solvents were procured from S.D. Fine Chemicals Limited, Sigma Aldrich USA, Mumbai, Hi Media, and Merck. Melting points were determined using the Thermo precision melting point cum boiling point (C-PMB) apparatus. Silica gel G-coated laboratory microslides were prepared through dipping to monitor TLC. The mobile phase used was a combination of polar and non-polar solvents in different quantities. The spots were detected using UV light and an iodine chamber. The IR spectra were recorded using a Bruker FT-IR spectrophotometer, which works on the KBr pellet technique. The 1H NMR spectra were

recorded on a Bruker 400 MHz NMR spectrometer with CDCl_3 as the solvent. High-resolution mass spectra were recorded on Micromass Q-TOF spectrometer using electrospray ionization.

Methods

Chemistry

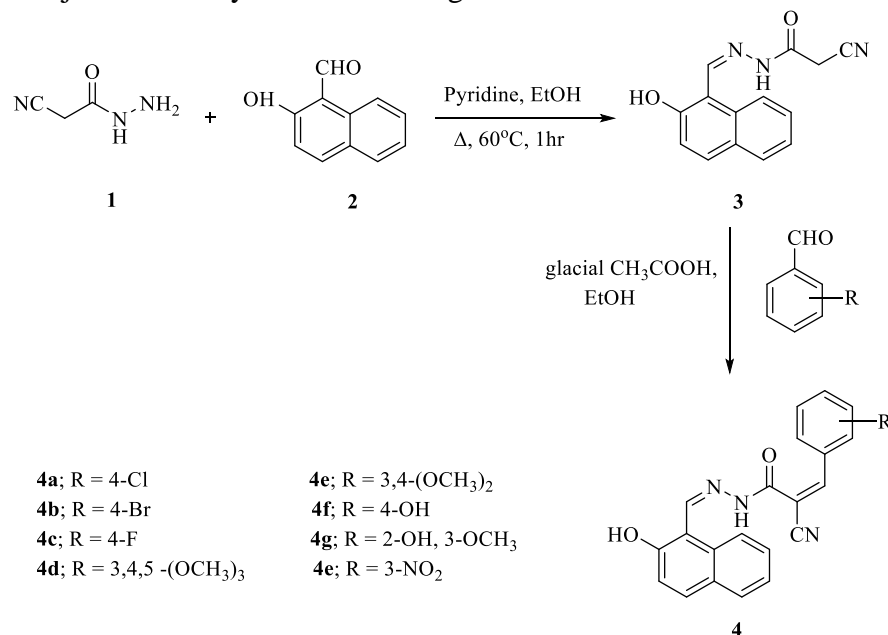
The formation of *N*-acyl hydrazide derivatives was achieved in 2 steps. In the first step, a reaction between an equimolar concentration of cyanoacetohydrazide (**1**) and 2-hydroxy-1-naphthaldehyde (**2**) through nucleophilic addition resulted in the formation of 2-cyano-*N'*-[(2-hydroxynaphthalen-1-yl)methylidene]acetohydrazide (**3**). In the next step, the Schiff base formed is reacted with substituted benzaldehydes (**4**) in equimolar concentrations, to form the final hydrazide derivatives via Knoevenagel condensation (Scheme).

Synthesis of 2-cyano-*N'*-[(2-hydroxynaphthalen-1-yl)methylidene]acetohydrazide (**3**)

0.01 mol of cyanoacetohydrazide was reacted with 0.01 mol of 2-hydroxy-1-naphthaldehyde, in a few amounts of ethanol and a few drops of pyridine. Then, this reaction mixture was refluxed at 60°Celsius for one hour. The reaction progress was monitored using TLC, and the resulting solid was collected, rinsed with water, and recrystallized using methanol.

General method for the synthesis of (Z)-2-cyano-*N'*-[(Z)-(2-hydroxynaphthalen-1-yl)methylene]-3-(substitutedphenyl)acrylohydrazides (**4a-4h**)

A solution containing 0.01 mol of 2-cyano-*N'*-[(2-hydroxynaphthalen-1-yl)methylidene]acetohydrazide (**3**), 0.01 mol of substituted benzaldehyde (**4**), a small amount of ethanol, and a few drops of glacial acetic acid was stirred for 4 hours. The reaction advancement was observed using thin-layer chromatography (TLC). The solid obtained was gathered, rinsed with water, and subjected to recrystallization using methanol.



Scheme. Synthesis of *N*-acyl hydrazide derivatives

Insilico Studies

Molinspiration

Molinspiration was used for the prediction of various physicochemical parameters that influence molecule activity, such as molecular weight, volume, Molecular Polar Surface Area (PSA), Hydrogen bond acceptor/donor, log P, and number of rotatable bonds, etc. Bioactivity score

indicates the overall potential of a compound to act as a drug candidate.

ADME properties

The ADME features of a molecule were assessed using Swiss ADME and PreADMET webtools, which predicted several aspects such as physicochemical properties, pharmacokinetics, drug-likeness, gastrointestinal (GI) absorption, blood-brain barrier permeability, skin permeability etc

Toxicity prediction

PreTox-II was used for the prediction of the toxicity of synthesized compounds, through which the estimated median Lethal Dose (LD50) in mg/kg body weight, oral toxicity, organ toxicity, carcinogenicity, and mutagenicity can be predicted.

Molecular docking

Molecular modeling provides insights into the structural and functional characteristics of proteins and ligands, whereas computational docking offers an estimation of binding affinities and the

binding modes, and types of interactions that exist in protein-ligand complexes. Molecular docking was performed using Autodock Vina 12.0 to obtain the best molecules among the title compounds, which can show potential antiinflammatory activity. The receptor COX-2 was chosen for its antiinflammatory activity. The structure of the COX-2 protein was taken from the Protein Data Bank (PDB ID: 5F19) and extracted to Autodock Vina. The ligand SMILES notations were collected from ChemsSketch upon drawing their structures, and these were converted to SDF formats using Open Babel. The SDF formats of the ligands are added to the Ligands section of Autodock Vina, and the ligands were docked with the protein. Celecoxib was taken as the inbuilt ligand or the standard ligand. The docking interactions were visually analyzed by Chimera Visualization Software.

Biological evaluation

Antiinflammatory activity - Carrageenan induced paw edema method

The *in vivo* inflammatory activity was performed only on four title compounds that were best docked against the COX-2 protein. The activity was evaluated using the carrageenan-induced hind paw edema test (Winter et al., 1962) in male albino rats (150–180 g) of the Wistar strain at 100 mg/kg body weight. Initially, the rats were divided into groups, each group containing 6 rats ($n = 6$). One group served as the control, and the second group, which received the standard drug, served as the standard/positive control. The other test groups were administered with the four test compounds, **4d-4g** respectively. The rats were administered orally with a dose of 100 mg/kg test compounds and celecoxib (positive control) or 10 ml/kg 0.5% sodium carboxymethyl cellulose (vehicle control) orally. This was done one hour before injecting 0.05 ml of 1% suspension of carrageenan into the subplantar region of the rat hind paw. A mark was created at the lateral malleolus of the right hind paw, and the foot was immersed to the same distance into the arm of the plethysmograph. Immediately, after injecting the carrageenan, the volume of the injected paw was assessed using water displacement in a plethysmograph.

The volume of the paw was measured once more after a period of 3 hours. The edema volumes of rats treated with the test substance and positive control were compared to those of the vehicle control animals. The comparison was done statistically and the results were expressed as the percentage of edema inhibition. The calculation of the percentage was done using a specific formula.

$$\text{Percentage edema inhibition} = 100(1 - V_t / V_c)$$

where, V_t = volume of edema in treated group,

V_c = volume of the edema in the control group.

After the experiment, one month washout period was allotted. Once the washout period had ended, the remaining 2 test compounds were administered in the same process mentioned earlier, and the evaluation was performed.

Antioxidant activity

Oxidative stress is a significant factor in the development of several diseases, notably cancer, alcoholic liver cirrhosis, and atherosclerosis. It is triggered by reactive oxygen species (ROS), like superoxide anion (O_2^-), perhydroxy radical ($HOO\cdot$), and hydroxyl radical ($OH\cdot$). The formation of these radicals occurs through a process of reducing molecular oxygen (O_2) by one electron (Braca et al., 2002; Maxwell, 1995). Reactive oxygen species (ROS) can readily trigger the process of lipid peroxidation in membrane lipids, resulting in damage to the cell membrane composed of phospholipids and lipoproteins through the propagation of a chain reaction cycle. Therefore, the antioxidant defense systems have evolved in conjunction with aerobic metabolism in order to mitigate the oxidative damage caused by reactive oxygen species (ROS) (Niki et al., 2008).

DPPH assay

The assessment of the 1,1-diphenyl-2-picrylhydrazyl (DPPH) scavenging activity was conducted using the method Blouin (1958). Test samples of concentration $100\mu M$ were mixed with $100\mu M$ DPPH in 95% ethanol and left at room temperature for 20 minutes. Then, the absorbance was measured at a wavelength of 517 nm. Ascorbic acid impact on DPPH was also evaluated for comparing it with the samples. The antioxidant substance converts the purple colored DPPH free radical back to the light yellow colored DPPH due to its proton donating tendency (Babu et al., 2001). Results are exposed as means of triplicate. The percentage inhibition was calculated by the formula:

$$\% \text{ Inhibition} = (\text{Absorbance of control} - \text{Absorbance of test} / \text{Absorbance of control}) \times 100$$

Nitric Oxide (NO) assay (Maccocci et al., 1994)

$100\mu M$ concentration of the methanolic solutions of test compounds were treated with $10\mu M$ sodium nitropruside in phosphate buffer at pH 7.4. and then incubated at $25^\circ C$ for 120 minutes. A control experiment was conducted in a similar way with same amount of solvent, but without the test compound. Instead, an equal amount of solvent was used. From this, 2mL was extracted and then mixed with 2mL of Griess reagent (Halliwell et al., 1987). The absorbance of the chromophore produced during diazotization of nitrite with sulphanilamide and subsequent addition of naphthylethylene diamine was taken at a wavelength of 546 nm. Additionally, the percentage of inhibition was also determined.

$$\% \text{ Inhibition} = (\text{Absorbance of control} - \text{Absorbance of test} / \text{Absorbance of control}) \times 100$$

Results and Discussion

Physicochemical data

(Z)-2-cyano-N'-((Z)-(2-hydroxynaphthalen-1-yl)methylene)-3-(4-chlorophenyl)acrylohydrazide (4a)

% Yield: 65%; Molecular Formula: $C_{21}H_{14}ClN_3O_2$; Melting Point: $150-152^\circ C$; Rf Value: 0.22; MP=Ethylacetate:n-Hexane (1:2); UV: 324nm; FTIR (KBr, cm^{-1}): 3201.73 (N-H), 3092.46 (Ar-H), 2258.20 ($C\equiv N$), 1678.03 ($C=O$), 1580.71 ($C=C$); 1H -NMR (400 MHz, $CDCl_3$) δ (ppm): 7.38-8.08 (m, 10H, Ar-H), 8.11 (s, 1H, vinylic CH), 8.72 (s, 1H, Imine -CH), 11.58 (s, 1H, NHCO), 12.19 (1H, bs, OH) Mol. Wt.: 375.81.

(Z)-2-cyano-N'-((Z)-(2-hydroxynaphthalen-1-yl)methylene)-3-(4-bromophenyl)acrylohydrazide (4b)

% Yield: 60%; Molecular Formula: $C_{21}H_{14}BrN_3O_2$; Melting Point: $168-169^\circ C$; Rf Value: 0.28; MP=Ethylacetate:n-Hexane (1:2); UV: 330nm; FTIR (KBr, cm^{-1}): 3248.32 (N-H), 3012.56 (Ar-

H), 2297.03 (C≡N), 1657.33 (C=O), 1516.21 (C=C); ¹H-NMR (400 MHz, CDCl₃) □ (ppm): 7.42-8.02 (m, 10H, Ar-H), 8.10 (s, 1H, vinylic CH), 8.70 (s, 1H, Imine -CH), 11.56 (s, 1H, NHCO), 12.25 (1H, bs, OH); Mol. Wt.: 420.26

(Z)-2-cyano-N'-((Z)-(2-hydroxynaphthalen-1-yl)methylene)-3-(4-fluorophenyl)acrylohydrazide (4c)

% Yield: 62%; Molecular Formula: C₂₁H₁₄FN₃O₂; Melting Point: 145-146⁰C; Rf Value: 0.22; MP = Ethylacetate:n-Hexane (1:2); UV:316nm; FTIR (KBr, cm⁻¹): 3291.16 (N-H), 3085.23 (Ar-H), 2247.13 (C≡N), 1625.12 (C=O), 1530.16 (C=C); ¹H-NMR(400 MHz, CDCl₃) □ (ppm): 7.45-8.01 (m, 10H, Ar-H), 8.16 (s, 1H, vinylic CH), 8.71 (s, 1H, Imine -CH), 11.51 (s, 1H, NHCO), 12.23 (1H, bs, OH); Mol. Wt.: 359.35

(Z)-2-cyano-N'-((Z)-(2-hydroxynaphthalen-1-yl)methylene)-3-(3,4,5-trimethoxyphenyl)acrylohydrazide (4d)

% Yield: 80%; Molecular Formula: C₂₄H₂₁N₃O₅; Melting Point: 192-193⁰C; Rf Value: 0.5; MP=Ethyl acetate :n-Hexane (1:2); UV:358nm; FTIR (KBr, cm⁻¹): 3368.20 (N-H), 3026.40 (Ar-H), 2828.68 (O-CH₃), 2258.10 (C≡N), 1682.50 (C=O), 1575.86 (C=C); ¹H-NMR (400 MHz, CDCl₃) □ (ppm): 3.96 (s, 6H, 2OCH₃), 3.84 (s, 3H, OCH₃), 6.73-8.02 (m, 8H, Ar-H), 8.11 (s,1H, vinylic CH), 8.68 (s, 1H, Imine -CH), 11.49 (s, 1H, NHCO), 12.21 (1H, bs, OH); MS(m/z): 432.23 (M+1)⁺, 433.29 (M+2)⁺; Mol. Wt.: 431.44.

(Z)-2-cyano-N'-((Z)-(2-hydroxynaphthalen-1-yl)methylene)-3-(3,4-dimethoxyphenyl)acrylohydrazide (4e)

% Yield: 80%; Molecular Formula: C₂₃H₁₉N₃O₄; Melting Point: 260-261⁰C; Rf Value: 0.4; MP=Ethylacetate:n-Hexane (1:2); UV:349nm; FTIR (KBr, cm⁻¹): 3384.01 (N-H), 3080.12 (Ar-H), 2824.16 (O-CH₃), 2288.96 (C≡N), 1642 (C=O), 1587 (C=C); ¹H-NMR (400 MHz, CDCl₃) □ (ppm): 3.97 (s, 6H, 2 OCH₃), 6.99-8.04 (m, 9H, Ar-H), 8.16 (s, 1H, vinylic CH), 8.72 (s, 1H, Imine -CH), 11.51 (s, 1H, NHCO), 12.17 (1H, bs, OH); Mol. Wt.: 401.41

(Z)-2-cyano-N'-((Z)-(2-hydroxynaphthalen-1-yl)methylene)-3-(4-hydroxyphenyl)acrylohydrazide (4f)

% Yield: 73%; Molecular Formula: C₂₁H₁₅N₃O₃; Melting Point: 144-145⁰C; Rf Value: 0.8; MP=Ethylacetate:n-Hexane (1:2); UV:341nm; FTIR (KBr, cm⁻¹): 3573.79 (O-H), 3301.20 (N-H), 3021.58 (Ar-H), 2298.12 (C≡N), 1632.01 (C=O), 1570.60 (C=C); ¹H-NMR (400 MHz, CDCl₃) □ (ppm): 6.51-8.06 (m, 10H, Ar-H), 8.14 (s, 1H, vinylic CH), 8.69 (s, 1H, Imine -CH), 9.55 (s, 1H, ph-OH), 11.56 (s, 1H, NHCO), 12.22 (1H, bs, OH); Mol. Wt.: 357.36

(Z)-2-cyano-N'-((Z)-(2-hydroxynaphthalen-1-yl)methylene)-3-(2-hydroxy-3-methoxyphenyl)acrylohydrazide (4g)

% Yield: 78%; Molecular Formula: C₂₂H₁₇N₃O₄; Melting Point: 182-184⁰C; Rf Value: 0.6; MP=Ethylacetate:n-Hexane (1:2); UV:362nm; FTIR (KBr, cm⁻¹): 3573.79 (O-H), 3346.52 (N-H), 3116.20 (Ar-H), 2898.02 (O-CH₃), 2302.16 (C≡N), 1698.02 (C=O), 1570.60 (C=C); ¹H-NMR(400 MHz, CDCl₃) □ (ppm): 3.85 (s, 3H, OCH₃), 6.63-8.05 (m, 9H, Ar-H), 8.13 (s,1H, vinylic CH), 8.65 (s, 1H, Imine -CH), 11.48 (s, 1H, NHCO), 12.25 (1H, bs, OH), 13.31(s, 1H, Ph-OH); Mol. Wt.: 387.39

(Z)-2-cyano-N'-((Z)-(2-hydroxynaphthalen-1-yl)methylene)-3-(3-nitrophenyl)acrylohydrazide (4h)

% Yield: 80%; Molecular Formula: C₂₁H₁₄N₄O₄; Melting Point: 210-213⁰C; Rf Value: 0.54; MP=Ethylacetate:n-Hexane (1:2); UV:303nm; FTIR (KBr, cm⁻¹): 3292.94 (N-H), 3082.68 (Ar-H), 2376.65 (C≡N), 1670.07 (C=O), 1576.96 (C=C), 1358.09 (NO₂); ¹H-NMR (400 MHz, CDCl₃) □ (ppm): 7.84-8.07 (m, 10H, Ar-H), 8.17 (s, 1H, vinylic CH), 8.74 (s, 1H, Imine -CH), 11.54 (s, 1H, NHCO), 12.24 (1H, bs, OH); MS(m/z): 387.10 (M+1)⁺, 388.06 (M+2)⁺; Mol. Wt.: 387.39

386.36

All the compounds were produced in satisfactory yields, ranging from 60–80%. The IR spectra of the compounds (**4a–4h**) exhibited bands in the range of 3384–3201 cm^{-1} indicating the presence of the NH functional group. The peaks that appeared between 2376–2247 cm^{-1} confirm the presence of the CN group. Further, the bands observed at 1682–1625 cm^{-1} correspond to C=O stretching, and those at 1580–1516 cm^{-1} were attributed to C=C stretching. The structural elucidation of the compounds was further done based on the observations of the ^1H NMR. The ^1H NMR spectra displayed a multiplet at δ 6.51–8.08 ppm for the aromatic protons. The CH=N–protons and –NHCO protons appeared as singlets at δ 8.68–8.74 ppm and 11.48–11.56 ppm, respectively. The mass spectra of molecules **4d** and **4h** exhibited peaks at m/z 432.23 (M+1)⁺ and 387.10 (M+1)⁺, respectively.

Insilico Studies

Molinspiration

With the aid of molinspiration, the molecular properties like hydrogen bond donors (HBD), hydrogen bond acceptors (HBA), Molar Refractivity (MR), Topological Polar Surface Area (TPSA), partition coefficient (Log $P_{o/w}$), number of Lipinski Violations (LV) were determined for the title compounds (Table 1).

Table 1. Molecular properties of compounds 4a-4h

Compound	HBA	HBD	MR	TPSA	Log $P_{o/w}$	LV
4a	4	2	106	85.5	2.96	0
4b	4	2	109	85.5	3.09	0
4c	5	2	101	85.5	2.79	0
4d	7	2	121	113	2.91	0
4e	6	2	114	104	3.07	0
4f	5	3	103	106	2.42	0
4g	6	3	110	115	2.86	0
4h	6	2	110	131	2.44	0

Table 1 reveals that all the compounds have desirable molecular properties and there are no Lipinski Violations for any compound.

ADMET Properties

The novel hydrazides **4a-4h** displayed high GI absorption, without BBB permeation and had 100% plasma protein binding capacity. The title compounds are inhibitors of certain Cytochromes, thereby majority of drug interactions incidence is less.

PreTox-II revealed that all the compounds are safe and non-toxic towards oral toxicity, organ

toxicity, mutagenicity, and carcinogenicity.

Molecular docking

Molecular docking was performed with the COX-2 protein (PDB ID: 5F19) and the results are tabulated in Table 2.

The standard drug celecoxib showed the docking score of -11.3 kcal/mol (Abdu-Allah et al., 2020) and the four derivatives, **4d-4g** exhibited comparable docking results to the standard. The dimethoxy (**4e**) derivative revealed a docking score of -11.7 kcal/mol, which is marginally superior to the standard whereas trimethoxy (**4d**), 2-hydroxy-3-methoxy (**4g**), and 4-hydroxy (**4f**) derivatives displayed good binding affinity with docking scores of -10.9 kcal/mol, -9.3 kcal/mol, and -8.2 kcal/mol, respectively, comparable to the inbuilt ligand. The derivatives interacted with various amino acids of the target protein, which facilitated the improvement of the binding energies and affinities of the compounds with the target. Based on these results, four hydrazide derivatives (**4d-4g**) were chosen for the *in vivo* antiinflammatory activity. Molecular docking of the derivatives **4d** and **4e** which exhibited excellent docking scores are shown in Figures 2&3.

Table 2. Molecular docking scores of compounds 4a-4h

Compound	XP - G Score (Kcal/mol)	Interacting amino acids
Celecoxib	-11.3	ARG, TYR, LEU, GLY
4a	-6.8	ARG, TYR, PRO, SER
4b	-6.5	TYR, PRO, ASN, CYS, HIS, GLY
4c	-6.4	TYR, LEU, GLY
4d	-10.9	TYR, GLY, ASN, PHE, LEU
4e	-11.7	TRPY, SER, GLY, LEU, ARG
4f	-8.2	LEU, SER
4g	-9.3	ARG, HIS, SER
4h	-7.2	PHE, LEU

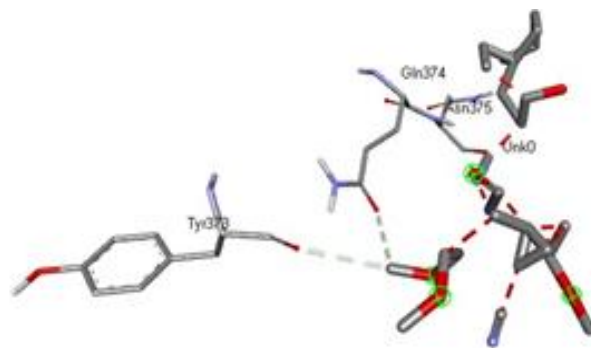


Figure 2. Molecular docking of **4d** with COX-2 protein

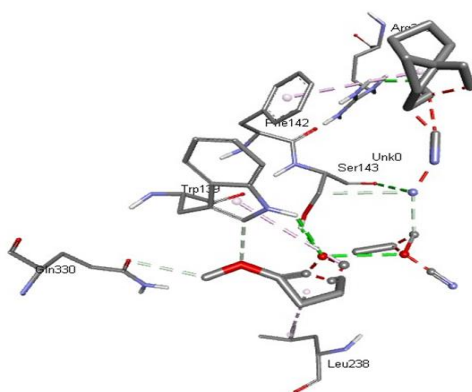


Figure 3. Molecular docking of **4e** with COX-2 protein

Biological evaluation

Antiinflammatory activity

Based on the docking results, the compounds, viz., **4d-4g**, were screened for *in vivo* antiinflammatory activity by the carrageenan-induced edema assay in rats (dose 100 mg/kg), and the data is shown in Table 3.

Table 3. The *in vivo* antiinflammatory activity of compounds **4d-4g**.

Compound	V _c	V _t	% Inhibition
4d	NA	0.2	78%
4e	NA	0.3	75%
4f	NA	0.4	67%
4g	NA	0.3	75%
Celecoxib	NA	0.2	78%

Vehicle (Control) 1.2 NA NA

* Significance levels *p < 0.5, **p < 0.01 and ***p < 0.001 by Dunnett's t-test

The *in vivo* study included initial recordings of paw volume prior to the administration of the drug and carrageenan. Subsequently, the paw edema volume was measured after the injection of carrageenan, marking the onset of inflammation. The final readings were noted after 3 hrs of inflammation. The percentage inhibitions were calculated for each derivative and are compared with that of standard.

The trimethoxy derivative (**4d**) showed similar activity to celecoxib, whereas the dimethoxy (**4e**), 2-hydroxy-3-methoxy (**4g**), and 4-hydroxy (**4f**) derivatives exhibited good anti-inflammatory activity.

Antioxidant activity

DPPH Assay

The results of the test compounds are tabulated in Table 4.

Table 4. DPPH assay results of compounds 4a-4h.

S.No.	Compound	% Inhibition at 100µM
1	4a	19%
2	4b	15%
3	4c	21%
4	4d	57%
5	4e	66%
6	4f	50%
7	4g	71%
8	4h	30%
9	Ascorbic Acid	88%
10	Control	-

All the synthesized compounds (**4a-4h**) were made to react with DPPH at a 100µM concentration and were estimated for the reduction of stable free radical DPPH to evaluate *in vitro* antioxidant activity. DPPH is a relatively stable free radical that determines the potentiality of synthesized compounds to reduce DPPH radicals by converting the unpaired ones to paired ones. Table 4 shows the reactivities of test compounds with DPPH at a 100 µM concentration. The absorbance was measured at a wavelength of 517 nm.

The data revealed that the 2-hydroxy-3-methoxy derivative (**4g**) showed a good and profound antioxidant activity of 71%. The 3,4,5-trimethoxy (**4d**) and 3,4-dimethoxy derivatives (**4e**) displayed moderate antioxidant activity with 57% and 66%, respectively. The 4-hydroxy

hydrazide derivative (**4f**) showed significant antioxidant activity of 50%, while the rest of the compounds showed less antioxidant activity (10%–30%).

Nitric Oxide Assay

Table 5 displays the potential of the test compounds to scavenge nitric oxide at a concentration of 100 μ M. The assay is based on the concept that sodium nitroprusside readily generates nitric oxide in an aqueous solution at physiological pH. The oxygen then reacts with the formed nitric oxide to generate nitrite ions, which can be quantified using Griess reagent. Nitric oxide scavengers compete with oxygen, leading to a decrease in nitrite ion concentration. The absorbance of the chromophore produced in the course of nitrite diazotization by the reaction with sulfanilamide, and its subsequent coupling with naphthyl ethylene diamine was measured at a wavelength of 546 nm.

The NO assay findings indicated that the 2-hydroxy-3-methoxy (**4g**) and 3,4-dimethoxy (**4e**) derivatives showed significant antioxidant activity of 56% and 52%, respectively, compared to the standard ascorbic acid's 67%. The 3,4,5-trimethoxy derivative (**4d**) displayed moderate antioxidant activity of 44%, while all other compounds showed less antioxidant activity (10% - 40%).

Table 5. NO scavenging assay results of compounds 4a-4h.

S.No.	Compound	% Inhibition at 100 μ M
1	4a	17%
2	4b	10%
3	4c	12%
4	4d	44%
5	4e	52%
6	4f	38%
7	4g	56%
8	4h	21%
9	Ascorbic Acid	67%
10	Control	NA

Conclusions

In conclusion, a series of *N*-acyl hydrazide derivatives (**4a–4h**) were synthesized. Molecular docking studies revealed that the compound **4e** have more affinity with the COX-2 protein compared to celecoxib while the compounds **4d**, **4f**, and **4g** exhibited less but comparable affinity with the COX-2 protein. All the compounds obeyed the Lipinski rule of five and showed good absorption and bioavailability. The *in vivo* anti-inflammatory results showed that the compound **4d** (trimethoxy) has comparable activity, and **4e**, **4f**, and **4g** exhibited less activity than that of celecoxib. The compound **4g** displayed good antioxidant activity in both DPPH and nitric oxide assays, while the compound **4e** exhibited better activity in the NO assay.

Acknowledgement

We greatly acknowledge SPMVV DBT-Builder project (Level-1) (BT/INF/22/SP47632/2023), for granting financial support for the upgradation of Animal House facilities and Sri Padmavati Mahila Visvavidyalayam, Tirupati for providing financial assistance under SEED MONEY grant (dated 31.01.2024) to carry out this research work smoothly.

Conflict of Interest

Authors declare no conflict of interest

References

1. Zarafu, I., Matei, L., Bleotu, C., Ionita, P., Tatibouët, A., Păuna, A., Nicolau, I., Hanganu, A., Limban, C., Nuta, D.C., Nemeş, R.M., Diaconu, C.C., and Radulescu, C. (2020). Synthesis, characterization, and biological activity of new acyl hydrazides and 1,3,4-oxadiazole derivatives. *Molecules*, 25(14), 3308. <https://doi.org/10.3390/molecules25143308>
2. Smith, P.A.S. (1951). *Organic Reactions*. (3rd Vol.) Moscow: Foreign Literature Publishers.
3. Ken-Ichi, O., Atsushi, T., Kosuke, T., Yuki, D., and Naoki, T. (2015). Hydrazidase, a novel amidase signature enzyme that hydrolyzes acylhydrazides. *J. Bacteriol.* 197(6), 1115–1124. <https://doi.org/10.1128/jb.02443-14>
4. Elnagdi, M. H., Erian, A. W. W. (1991). New routes to polyfunctionally substituted pyridine, pyridopyridine, quinoline, and pyridazine derivatives. *Arch. Pharm.* 324(11), 853–858. <https://doi.org/10.1002/ardp.2503241106>
5. Sambrajyam, J., Vidya Rani, M., and Rajitha, G. (2022). Synthesis, molecular docking and biological evaluation of naphthyl N-acyl hydrazone derivatives. *Asian J. Chem.* 34(7), 1675–1682. <https://doi.org/10.14233/ajchem.2022.23632>
6. Soujanya, M. and Rajitha, G. (2017). Synthesis, characterization, molecular docking and antimicrobial activity of nicotinic acid derived N-acylhydrazones. *Der. Pharma. Chemica.* 9(17), 10–15. <https://doi.org/10.3390/ijms23052823>
7. Hegira, R., Esteban, F., Juan, R., Soriuska, M., Gricelis, M., Carmen, C., De Sanctis, J.B., Mijares, M., and Charris, J. (2021). Synthesis and antimalarial and anticancer evaluation of 7-chloroquinoline-4-thiazoleacetic derivatives containing aryl hydrazide moieties. *Arch. Pharm.* 354(7), 202100002. <https://doi.org/10.1002/ardp.202100002>
8. Wagdy, M.E., Mohamed, F., Marwa, M.A.A., and Hatem, A.A.A. (2015). Design, synthesis and antitubercular activity of certain nicotinic acid hydrazides. *Molecules*, 20(5), 8800–8815. <https://doi.org/10.3390/molecules20058800>
9. Vikramjeet, J., Balasubramanian, N., Munish, A., Dharmarajan, S., Perumal, Y., Erik De, C., Pannecouque, C., and Balzarini, J. (2013). Synthesis, antimycobacterial, antiviral, antimicrobial activity and QSAR studies of N²-acyl isonicotinic acid hydrazide derivatives. *J. Med. Chem.* 9(1), 53–76. <http://dx.doi.org/10.2174/1573406411309010053>
10. Vikas, N.T., Anirudh, B., Vinod Kumar, B., and Kalpana, S. (2012). Novel N'-benzylidene benzofuran-3-carbohydrazone derivatives as antitubercular and antifungal agents. *Bioorg. Med. Chem. Lett.* 22(6), 2343–2346. <https://doi.org/10.1016/j.bmcl.2012.01.067>
11. Zahid, H.C., and Hazoor, A.S. (2008). Structural elucidation and biological significance of 2-hydroxy-1-naphthaldehyde derived sulfonamides and their first row d-transition metal chelates. *J. Enzyme Inhib. Med. Chem.* 23(3), 369–379. <https://doi.org/10.1080/14756360701585692>
12. Sarah, F.J., Emmanuel, A., Ngan, P.H., Curtis, R.C., Peihua, G., Jiangbing, Z., Zhang, Y., Graviss, E.A., Liu, J.O., and Olaleye, O.A. (2016). Characterization of 2-hydroxy-1-

naphthaldehyde isonicotinoylhydrazone as a novel inhibitor of methionine aminopeptidases from mycobacterium tuberculosis. *Tuberculosis*. 101,73–77.

<https://doi.org/10.1016/j.tube.2016.09.025>

13. Neelofar, N., Ali, N., Khan, A., Amir, S., Amir Khan, N., and Bilal, M. (2018). Synthesis of schiff bases derived from 2-hydroxy-1-naphthaldehyde and their tin (II) complexes for antimicrobial and antioxidant activities. *Bull Chem Soc Ethiop*. 31(3), 445–56.
<http://dx.doi.org/10.4314/bcse.v31i3.8>
14. Bhagwat, V., Digambar, K., and Avinash, S. (2022). Synthesis, spectral studies, antioxidant and antibacterial evaluation of aromatic nitro and halogenated tetradentate schiff bases. *Heliyon*. 8(6), e09650. <https://doi.org/doi: 10.1016/j.heliyon.2022.e09650>.
15. Winter, C., Risley, E., and Nus, G. (1962). Carrageen-induced edema in hind paw of the rat as an assay for anti-inflammatory drugs. *Proc. Soc. Exp. Biol. Med.* 111(3), 544–547.
<https://doi.org/doi: 10.3181/00379727-111-27849>
16. Braca, A., Sortino, C., Politi, M., Morelli, I., and Mendez, J. (2002). Antioxidant activity of flavonoids from *Licania licaniaeflora*. *J. Ethnopharmacol.* 79(3), 379–381. [https://doi.org/10.1016/S0378-8741\(01\)00413-5](https://doi.org/10.1016/S0378-8741(01)00413-5)
17. Maxwell, S. R. (1995). Prospects for the use of antioxidant therapies. *Drugs*, 49(3), 245–361.
18. Niki, E., Shimaski, H., and Mino, M. (2008). Antioxidantism-free radical and biological defence. *Gakkai Syuppn Center*. Tokyo, 1994.
19. Blios, M. S. (1958). Antioxidant determinations by the use of stable free radical. *Nature*. 181, 1199–1200. <https://doi.org/10.1038/1811199a0>
20. Babu, B. H., Shylesh, S., Padikkala, J. (2001). Antioxidant and hepatoprotective effect of *Acanthus ilicifolius*. *Fitoterapia*. 72 (3), 272–277. [https://doi.org/10.1016/S0367-326X\(00\)00300-2](https://doi.org/10.1016/S0367-326X(00)00300-2)
21. Marcocci, L., Maguire, J. J., Droy-Lefaix, M. T., and Packer, L. (1994). The Nitric oxide scavenging properties of Ginkgo Biloba extract Egb 761. *Biochem. Biophys. Res. Commun.* 201(2), 748–755. <https://doi.org/10.1006/bbrc.1994.1764>
22. Halliwell, B., Gutteridge, J. M. C., and Aruona, O. I. (1987). The deoxyribose method: A sample test tube assay for determination of rate constants for reactions of hydroxyl radicals. *Anal. Biochem.* 165(1), 215–219. [https://doi.org/10.1016/0003-2697\(87\)90222-3](https://doi.org/10.1016/0003-2697(87)90222-3)
23. Abdu-Allah, Hajja. H. M., Abdelmeoaz Alshaimaa, A. B., Tarazi, H., El-Shorbagi Abdel-Nasser A., and El-Awady, R. (2020). Conjugation of 4-aminosalicylate with thiazolinones afforded non-cytotoxic potent in vitro and in vivo anti-inflammatory hybrids. *Bioorg. Chem.* 94, 103378. <https://doi.org/10.1016/j.bioorg.2019.103378>